Silicon photomultiplier-based detection module with up to 1 cm2 area to push time-domain diffuse optics performances

Di Sieno, Laura, Dalla Mora, Alberto, Behera, Anurag, Gola, Alberto, Acerbi, Fabio

Laura Di Sieno, Alberto Dalla Mora, Anurag Behera, Alberto Gola, Fabio Acerbi, "Silicon photomultiplier-based detection module with up to 1 cm2 area to push time-domain diffuse optics performances ," Proc. SPIE 11920, Diffuse Optical Spectroscopy and Imaging VIII, 1192005 (9 December 2021); doi: 10.1117/12.2615204

SPIE.

Event: European Conferences on Biomedical Optics, 2021, Online Only

Silicon photomultiplier based detection module with up to 1 cm^2 area to push time-domain diffuse optics performances

Laura Di Sieno[1], Alberto Dalla Mora[1], Anurag Behera[1], Alberto Gola[2] and Fabio Acerbi[2]

[1] Politecnico di Milano, dipartimento di Fisica, Piazza Leonardo da Vinci 32, 20133 Milano (MI)
[2] Fondazione Bruno Kessler (FBK), Via Sommarive, 38123 Trento, Italy
Author e-mail address: laura.disieno@polimi.it

Abstract: We present the largest detectors for time-domain diffuse optics, showing superior performances in depth penetration and light-harvesting capability. *In-vivo* measurements demonstrate their potentialities for futuristic disruptive applications such as optical radiography.

1. Introduction

Recent years have witnessed an increasing interest in the use of Silicon PhotoMultipliers (SiPMs) for time-domain diffuse optics (TD-DO). Indeed, first SiPMs were used in 2015 [1] and were demonstrated to be suitable for several TD-DO applications [2–4]. With respect to traditional detectors (such as PhotoMultipliers Tube -PMTs- or Hybrid PMTs) they have the advantages of solid-state detectors (ruggedness, compactness, insensibility to electromagnetics field, etc.) while having a much higher light harvesting capability thanks to their area (about 1 mm^2) and the possibility to be put directly in contact with the sample under investigation, thus exploiting their whole numerical aperture. Nevertheless, to push the TD-DO towards its limit, it is of the utmost importance to further advance in two directions: i) the light harvesting capability; ii) the throughput of the timing electronics.

A first work showing the suitability of a larger area SiPM (active area of 7.38 mm^2) working beyond the limit of the pile-up statistics was published recently [4]. However, to open the way to new possible applications (e.g., monitoring of deep structure such as lungs or heart) as well as to approach the possibility to measure the chest in transmittance (the first step toward optical radiography) a much larger area detector is needed. In this work, we present the latest results in term of large area SiPMs specifically conceived for TD-DO measurements with an effective active area of about 32 mm^2 and its improved version with 92 mm^2 respectively. We assess the basic performances of both devices using the Basic Instrumental Performance (BIP) protocol [5]. Moreover, for the 32 mm^2 device, we evaluate its performances using well established protocols for performance assessment of DO instruments (namely, MEDPHOT and nEUROPt protocols [6,7]) and finally we tested it for first *in-vivo* acquisition.

2. Material and Methods

2.1 SiPM module and setup

The first device is a custom-made 6 x 6 mm^2 detector based on 4 SiPMs in parallel (dimension of the single chip: 3 x 3 mm^2, with 35 μm cell pitch) arranged in a square geometry to reach an overall effective active area of 32.1 mm^2. The device is based on VUV-HD technology [8], is cooled to about -15°C thanks to a 2-stage Peltier cooler and housed inside a vacuum TO8 package. On the other hand, the second large area SiPM is a nominal 1 cm^2 with 92 mm^2 active area detector, based on NIR-HD technology, segmented into 6 sub-SiPMs for better signal extraction and cooled to -36°C. The front-end electronics for avalanche reading is embedded in the module itself. The 32 mm^2 detector is biased at the operative voltage of 39 V (i.e., 6.8 V excess bias), while the 92 mm^2 is biased at 36 V (i.e., 8 V excess bias). Both detectors have been designed and realized in FBK (Trento, Italy).

The experimental setup is composed of a laser source (supercontinuum coupled to a rotating prism -SuperK Extreme, NKT Photonics- or a 670 nm high power diode laser -LDH-P-670 by Picoquant GmbH, Germany-) which emits light at given wavelength (one in the range from 600 to 1000 nm for the supercontinuum source or 670 nm for the diode laser) at a repetition rate of 40 MHz. The light is then attenuated by means of a variable optical attenuator and inject into the sample through a 600 μm-core optical fiber. Re-emitted photons are then collected putting the detector directly in contact with the sample. When a photon triggers an avalanche, an output signal provided by the module is fed to the time-correlated single-photon counting board (SPC-130, Becker and Hickl GmbH, Germany) while the stop signal is given by a synchronization signal provided by the laser driver simultaneously with the optical pulse.

Diffuse Optical Spectroscopy and Imaging VIII, edited by Davide Contini, Yoko Hoshi, Thomas D. O'Sullivan, Proc. of SPIE-OSA Vol. 11920, 1192005 · © 2021 OSA-SPIE
CCC code: 1605-7422/21/$21 · doi: 10.1117/12.2615204

2.2 Measurement and data analysis

To assess the performances of the detectors, first we apply some tests from the BIP protocol such as the responsivity (i.e., measurement of light harvesting capability) as well as the study of the Instrument Response Function (IRF). Those measurements were carried out in the whole spectral range (600 to 1000 nm at steps of 50 nm).

Moreover, for the 32 mm^2 device, we assessed the suitability of the realized detector to retrieve optical properties of homogeneous media at 670 nm (MEDPHOT protocol) as well as the capability to detect an optical perturbation buried into a diffusive medium (nEUROPt protocol). MEDPHOT protocol was implemented recovering the optical properties of the 32 phantoms spanning a wide range of optical properties (conventionally true values: absorption coefficient -μ_a- from 0.01 to 0.47 cm^{-1}, reduced scattering coefficient -μ_s'- from 7 to 20 cm^{-1}) and computing the linearity and the accuracy in the retrieval of μ_a and μ_s'. The source-detector distance (SDD) was set to 3 cm and optical properties were recovered by fitting the experimental data to the analytical model of the photon transport in a diffusive semi-infinite medium under the diffusion approximation.

nEUROPt protocol was performed by translating in depth (from 2.5 to 50 mm) a totally absorbing inclusion (equivalent to a $\Delta\mu_a$= 0.17 cm^{-1} over 1 cm^3 [9]) through a homogenous liquid phantom (μ_a= 0.1 cm-1; μ_s'= 10 cm^{-1}). The SDD was set at 8 cm. As dictated in [7], the contrast (i.e., relative change in the number of photons between the perturbed and unperturbed case) as well as the contrast-to-noise ratio -CNR- (i.e., the robustness of the contrast with respect to noise) was evaluated in time-gates (width: 1 ns, defined from the peak of the IRF).

As last test, we challenged the 32 mm^2 module with *in-vivo* measurements on different regions of the body to suggest the possible applications that will be enabled by such a large area detector. As a first step, we tested the maximum SDD that can be used on different regions of the body (namely, forehead, chest measured on a side, knee and shoulder) and, from the recorded curves, we recovered the μ_a values with the same procedure described for MEDPHOT protocol. Measurements were done on a healthy subject and were approved by the Ethical Committee of Politecnico di Milano and conducted in compliance with the Declaration of Helsinki.

3. Results, discussion and conclusions

The spectral responsivity of the 32 mm^2 detector is 10^{-5} m^2sr and $1.83\cdot10^{-7}$ m^2sr at 600 and 1000 nm respectively and it increases to $1.7\cdot10^{-5}$ and $7.7\cdot10^{-5}$ m^2sr for the 92 mm^2 one. The responsivity for the two devices is thus more than 1 decade higher with respect to state-of-the-art research instruments. Indeed, the system presented in Ref. [2] has a responsivity of $1.4\cdot10^{-7}$ m^2sr at 830 nm while the two proposed detectors feature at 850 nm $2\cdot10^{-6}$ m^2sr and $9.2\cdot10^{-6}$ m^2sr (32 and 92 mm^2 respectively). The improvement in responsivity increases to orders of magnitude when compared to state-of-the-art clinical systems ($3.3\cdot10^{-8}$ m^2sr at 820 nm) [10]. The IRF shape is depicted in Figure 1(a) for both detectors at 700 and 850 nm and it has no particular feature that may prevent the use in TD-DO, as will be better enlightened later with MEDPHOT and nEUROPt protocol.

The MEDPHOT protocol assesses the suitability of the detector to recover optical properties of homogenous medium. Considering phantoms with optical properties mimicking of human tissues (i.e., $\mu_a \leq 0.21$ cm^{-1} and μ_s'<15 cm^{-1}), we have an accuracy higher than 9% for absorption coefficient and 6% for the reduced scattering one. Moreover, the linearity in the retrieval of both μ_a and μ_s' was found to be in line with state-of-the-art devices (data not shown).

The contrast and CNR obtained from the nEUROPt protocol are reported in Fig. 1(b)-(c) for several time-gates. Points with CNR<1 (theoretical limit to distinguish contrast from noise) were removed from contrast plot. Using the 4-5 ns gate, the perturbation can be seen up to 38 mm where contrast reaches 1% (i.e., same order of biological fluctuations, thus variation lower than this value cannot be detected in real settings) with CNR >1.

The results of the *in-vivo* acquisitions are reported in Fig. 1(d). Thanks to the high responsivity of the detector, it was possible to have measurements with SDD of more than 10 cm (up to 13 cm for the chest) that still allows to recover a value of absorption coefficient that is compatible with biological tissues.

In conclusions, we presented 2 detectors with the largest light harvesting capability ever demonstrated and we verified, through well assessed protocols for performance assessment of TD systems, the suitability of one of them for recovering optical properties of homogeneous media. Additionally, we were able to detect a perturbation at the remarkable depth of 38 mm in standardized measurement conditions that, to the best of our knowledge, is the maximum penetration depth achieved by TD instruments. Indeed, in Ref [11] the same penetration depth was reached but using a more complex fast-gated SiPM. *In-vivo* measurements additionally show that large SDD can be used allowing the retrieval of absorption value. Further improvements to the achieved results are expected using the 92 mm^2 detector (measurements are currently in progress).

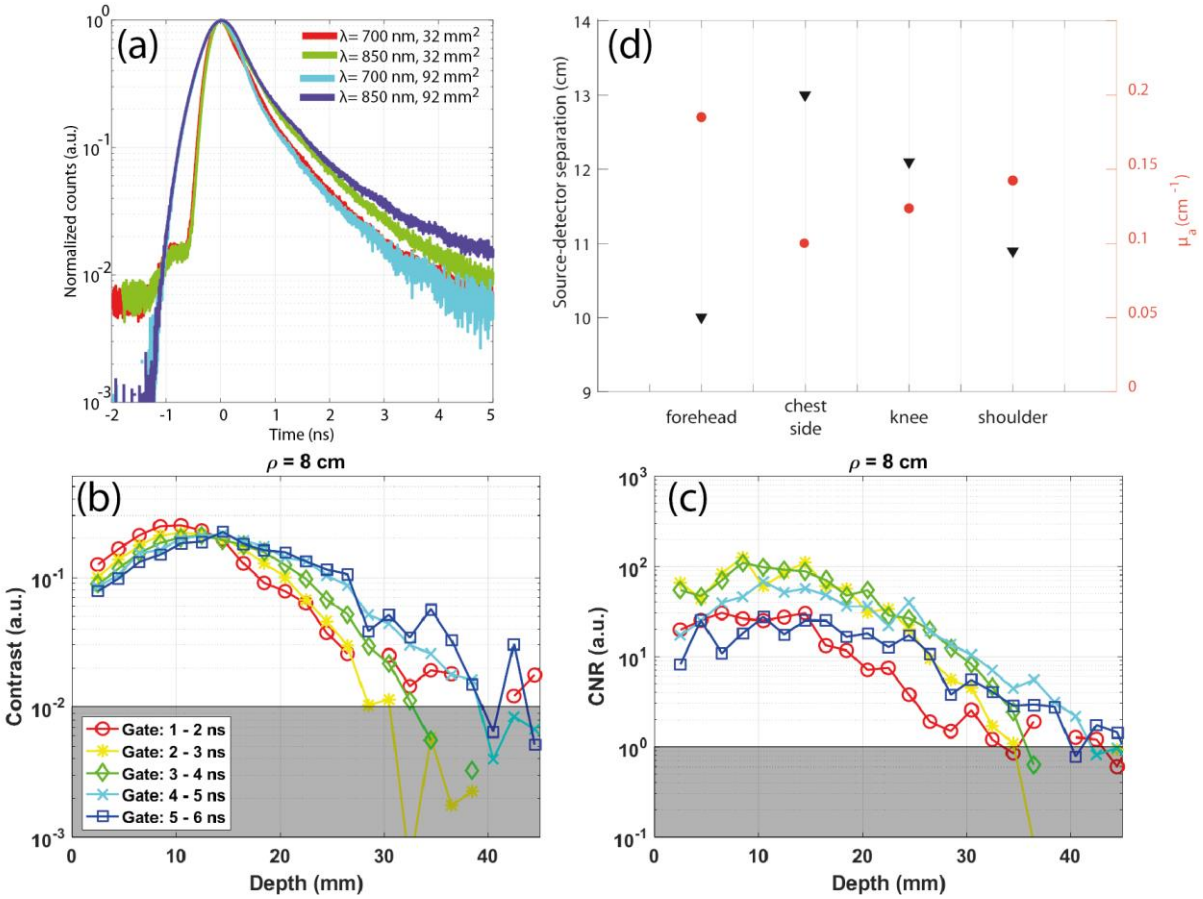

Fig. 1. (a) IRFs normalized in amplitude and time for 2 wavelengths (700 and 850 nm) for both devices. (b-c) contrast and CNR computed in different time-gates. (d) maximum SDD (left scale, black triangles) and retrieved value of μ_a (right scale, red circles) obtained in *in-vivo* measurements for different body regions.

Generally speaking, the new generation of large area SiPMs could allow to probe regions of the body usually considered not accessible (e.g., heart, lung etc) and will open the way to the measure the body in transmittance thus laying the foundation for optical radiography.

Acknowledgements

This research has received funding from the ATTRACT project funded by EU under grant agreement no 777222.

References

[1] A. Dalla Mora et al, "Fast silicon photomultiplier improves signal harvesting and reduces complexity in time-domain diffuse optics," Opt. Express 23, 13937–13946 (2015).
[2] R. Re et al, "Probe-hosted silicon photomultipliers for time-domain functional near-infrared spectroscopy: phantom and in vivo tests," Neurophotonics 3, 045004 (2016).
[3] L. Di Sieno et al., "Time-domain diffuse optical tomography using silicon photomultipliers: Feasibility study," J. Biomed. Opt. 21, (2016).
[4] L. Di Sieno et al., "Probe-hosted large area silicon photomultiplier and high-throughput timing electronics for enhanced performance time-domain functional near-infrared spectroscopy," Biomed. Opt. Express 11, 6389 (2020).
[5] H. Wabnitz et al., "Performance assessment of time-domain optical brain imagers, part 1: basic instrumental performance protocol," J. Biomed. Opt. 19, 86010 (2014).
[6] A. Pifferi et al., "Performance assessment of photon migration instruments: the MEDPHOT protocol.," Appl. Opt. 44, 2104–2114 (2005).
[7] H. Wabnitz et al., "Performance assessment of time-domain optical brain imagers, part 2: nEUROPt protocol," J. Biomed. Opt. 19, 86012 (2014).
[8] F. Acerbi et al., "Silicon Photomultipliers: Technology Optimizations for Ultraviolet, Visible and Near-Infrared Range," Instruments (2019).
[9] F. Martelli et al, "Phantoms for diffuse optical imaging based on totally absorbing objects, part 1: Basic concepts.," J. Biomed. Opt. 18, 066014 (2013).
[10] R. Re et al, "Multi-channel medical device for time domain functional near infrared spectroscopy based on wavelength space multiplexing," Biomed. Opt. Express **4**, 2231–2246 (2013).
[11] L. Di Sieno et al, "Time-domain diffuse optics with 8.6 mm² fast-gated SiPM for extreme light harvesting," Opt. Lett. 46, 424–427 (2021)